Impact of near-contact barriers on the subthreshold slope of short-channel CNTFETs

Martin Claus*,**, Stefan Blawid§ and Michael Schröter**,‡
* Center for advancing electronics Dresden, Technische Universität Dresden, Germany, Email: martin.claus@tu-dresden.de
** Department of Electrical Engineering and Information Technology, Technische Universität Dresden, Germany
‡ ECE Department, UC San Diego, USA, Email: mschroter@ieee.org
§ Department of Electrical Engineering, Universidade de Brasília, Brazil, Email: stefan@ene.unb.br

***Abstract*—Recent experimental investigations of sub-10 nm carbon nanotube (CNT) field-effect transistors (FETs) promote CNT based 1D-electronics as a candidate for a future aggressively scaled transistor technology. However, the ballistic transport within the 1D semiconducting CNT channel is largely determined by charge injection from the contacts rendering reliable theoretical predictions of the transistor performance difficult. Based on a simplified heterojunction like contact model, we demonstrate by solving the Schrödinger-Poisson equations that aggressive scaling will rely on a careful balance between two components of the injected charges, one responsible for the formation of near-contact barriers and the other carrying the current. Excellent electrostatic gate control (e.g. employing thin gate oxides) may then enable transistor scaling until the onset of direct source-drain tunneling.**

***Index Terms*—CNTFET, 1D-electronics, Schrödinger equation, quantum transport, subthreshold slope, short channel**

I. Introduction

Carbon nanotubes (CNTs) belong to a group of materials confining the current to one spatial dimension (1D) and thus offering exceptional unique intrinsic properties such as long mean free paths, high current carrying capability, high carrier velocity (up to $1 \times 10^8\,\mathrm{cm\,s^{-1}}$) and predicted THz performance [1]–[3]. Typical short channel effects as known from conventional silicon-based bulk MOSFETs are not expected for ultra-low-scaled CNTFETs. Along with their thermal ruggedness, CNTFETs are therefore very interesting for digital applications. However, a reliable fabrication method (especially in terms of reproducibility and intentional tube placement) of single-tube short-channel CNTFETs is very challenging and, so far, many problems are not solved. Thus, simulation based studies are needed, to improve the device understanding and to support the technology development. An overview on CNTFET technology can be found in [4].

Recently, experimental results for a 9 nm long CNTFET were published demonstrating excellent performance [5], which disprove for short channel CNTFETs two theoretical claims [6], [7]: (*i*) the drain current will not saturate due to drain-induced barrier lowering (DIBL) and (*ii*) the subthreshold slope (STHS) increases significantly for channel lengths below 15 nm due to a very high charge injection from the contacts into the channel. In [8] and [5] the discrepancy between the theoretical claims and the experimental results was explained with fringing fields from the gate that modulate the near-contact potential barriers in the experiments. In [5] it is argued that the modulation by the fringing fields effectively lengthens the channel while [8] explains this behavior by using top contacts instead of embedded contacts leading to a better gate control of the contact regions.

In this paper, the impact of the metal-CNT interface and the tube portion underneath the metal (i. e. the contact region) on the charge injection and, thus, on the overall transistor behavior is investigated. Especially, the second claim about the scaling behavior of the STHS is studied. By adjusting the model parameters describing the charge injection, a very good agreement between the experimental and the simulation results were obtained, thus providing an alternative explanation for the excellent scaling behavior of the sub-10 nm long CNTFET.

II. Model

A wide range of simulation approaches have been utilized for analyzing the properties and performance of CNTFETs, ranging from atomistic first-principles methods [9] over Schrödinger-Poisson [3], [7] and Boltzmann transport equation [10], [11] solvers to compact models (see e. g. [12] for an overview).

Of major concern in all simulation approaches is the treatment of the regions from where the charge carriers are injected into the channel (see [13] for an overview). In CNTFETs the carrier injection is significantly affected by the coupling strength between the contact metals and the CNT in the contact regions [14]. Chemical bonding between the contact metal atoms and the CNT atoms can alter the CNT band structure considerably [9] leading to a potential step at the interface between the contact regions and the channel (uncoated CNT portion) (see Fig. 1). We claim that the transition from the metal-coated tube portion to the uncoated tube portion can then be modeled as a heterojunction (see Fig. 1(b)) [3].

The potential step $\triangle E + \Phi_{\mathrm{sb}}$ at the interface implies that the wave functions of contact electrons with energies within the channel band gap will only weakly leak from the contact into the channel (similar to metal-induced gap states (MIGS)) (see Fig. 3). However, since the effective mass in CNTs is very low, the tunneling length is high leading to a significant carrier density concentrated nearby the contact regions. Considering the overall electrostatics, potential barriers close to the ends

978-1-4673-5736-4/13/$31.00 ©2013 IEEE

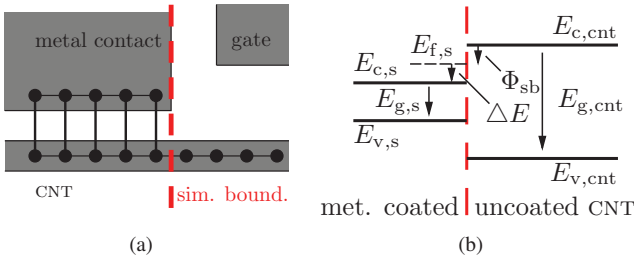

Fig. 1: **(a)** Schematic of the metal-CNT contact region and **(b)** band profile of the heterojunction in this region.

of the channel are formed in addition to the inherent potential step. Moreover, the channel length (i. e. the separation of the source and drain contact) determines the electrostatics and thus the bias-dependence of these barriers which suggests a noteworthy channel length dependence of the specific device figures of merit such as the STHS.

Although very valuable *per se*, a semi-classical approach with ohmic contacts (e. g. [15]) or even with Schottky-like contacts (e. g. [11]) can not elucidate and quantify the impact of metal-induced gap states on the behavior of short-channel CNTFETs since charge injection into the band gap is not possible within a semi-classical approach. Therefore, for the simulations in this paper, an in-house effective-mass Schrödinger-Poisson solver (COOS) [3] is used together with a heterojunction-based contact model [16] which allows to change the coupling strength and the height of the potential step at the interface between the contact regions and the channel. The simulation boundaries for the Poisson and the Schrödinger equation are set directly at the interfaces between the metal-coated and uncoated tube portion in the source and drain contact region (see Fig. 1(a)). For simplicity, the barrier at this interface is called Schottky barrier. The boundary conditions for the Poisson equation are set according to [17]. Note that we treat charge injection into the band gap as part of the self-consistency loop of charge and electrical potential calculation.

Low contact transparency due to insufficient wetting and additional carrier reflections at the bulk metal to CNT interface are likely to be bias independent and may be taken into account as series resistance or as constant current scaling [16].

III. Application

Fig. 2 compares the measured transfer characteristic of a 9 nm long CNTFET [5] with predicted characteristics simulated with the Schrödinger-Poisson solver COOS after adjusting the charge-injection parameters, the channel length and the tube diameter. All other parameters are identical to the structure described in [5]. The contact parameters (see [3] for an explanation) are $E_{v,\mathrm{eff}} = 0.4\,\mathrm{eV}$, $m^*_{s/d}/m_0 = 0.4$ and $\Phi_{sb,p} = 0.15\,\mathrm{eV}$ and the tube diameter equals 1.1 nm. For this parameter set, the best agreement with the experimental results was obtained for a channel length of 10 nm (instead of 9 nm in the experiment and 14 nm for the simulation results shown in [5]). The slightly longer channel employed in the simulation seems plausible since the potential barriers at the ends of the channel will extend slightly into the contact regions which is not considered in the approach described here. (Note that the claimed STHS of $94\,\mathrm{mV\,dec^{-1}}$ in [5] could not be verified for the experimental data given in [5]. Instead, a value of around $115\,\mathrm{mV\,dec^{-1}}$ was extracted from the experimental results along the studies for this paper.)

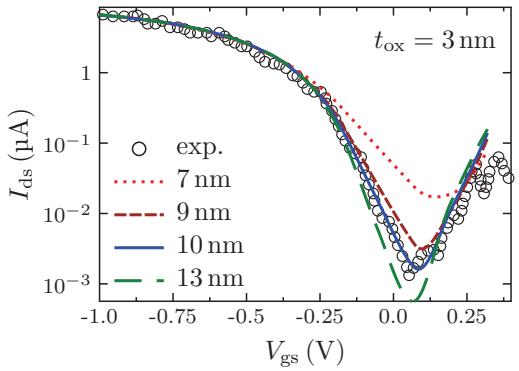

Fig. 2: Comparison between experimental results [5] of a 9 nm long CNTFET and simulation results for various channel lengths and $V_{ds} = -0.4\,\mathrm{V}$.

The valence band along the channel for the 10 nm long CNTFET is shown in Fig. 3(a) for $V_{ds} = -0.4\,\mathrm{V}$ and several V_{gs}. Obviously, even for negative gate voltages, the top of the source-sided potential barrier is above the nominal Schottky barrier of 0.15 eV due to the carrier leaking into the channel band gap. Fig. 3(b) shows the contour plot of the energy-dependent hole spectrum $\mathcal{P}^+$ injected from the source contact region for $V_{gs} = -0.25\,\mathrm{V}$. According to this figure the peak of the carrier concentration injected from the source contact region remains nearby the source and within the band gap. For the carriers injected from the drain region (not shown here), the related carrier concentration reaches its maximum also close to the contact region from where the carriers originate. The peaks at the ends of the channel lead to the aforementioned potential barriers.

Since COOS solves the effective-mass Schrödinger equation for calculating the charges and the current, the underlying band structure is parabolic which can lead to effective carrier velocities above the Fermi velocity v_f which in turn may lead to unrealistic results. Indeed, as shown in Fig. 4, the energy-dependent effective velocity $\mathcal{V}^+_{p,\mathrm{eff}}$ of the carriers $\mathcal{P}^+$ injected from the source contact region

$$\mathcal{V}^+_{p,\mathrm{eff}}(E,x) = \frac{\mathcal{I}^+_p(E)}{q\,\mathcal{P}^+(E,x)} \tag{1}$$

can exceed the Fermi velocity v_f ($\mathcal{I}^+_p$ is the related hole current injected from the source contact region). However, for the shown bias point, the velocity excess does not impact the current and charge calculation since it is outside of the relevant

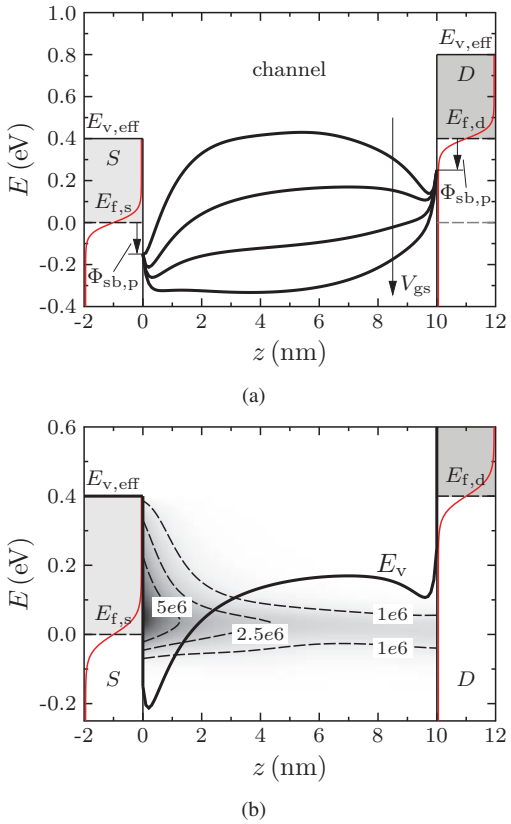

Fig. 3: **a)** Valence band profile for several gate voltages ($V_{\mathrm{gs}} = 0.375$, 0.125, -0.25 and $-0.875\,\mathrm{V}$) and $V_{\mathrm{ds}} = -0.4\,\mathrm{V}$ and **b)** contour plot of the energy-dependent hole density $\mathcal{P}^{+}$ in units of $\mathrm{cm}^{-1}\,\mathrm{eV}^{-1}$ for $V_{\mathrm{gs}} = -0.25\,\mathrm{V}$ and $V_{\mathrm{ds}} = -0.4\,\mathrm{V}$. The red curves in the contact regions show the Fermi function at 300 K.

charge and current energy intervals (see Fig. 3). Thus, non-parabolic effects are not important for the investigated device figures of merit in this paper.

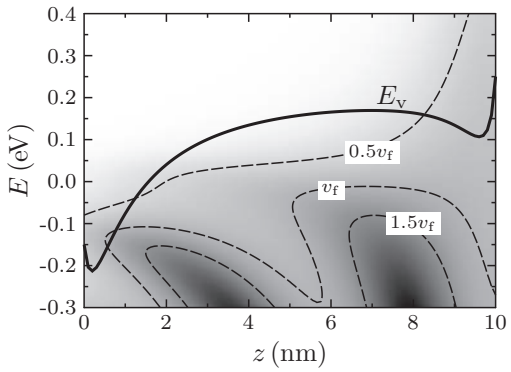

Fig. 4: Contour plot of the energy-dependent effective velocity $\mathcal{V}_{\mathrm{p,eff}}$ along the channel for $V_{\mathrm{gs}} = -0.25\,\mathrm{V}$ and $V_{\mathrm{ds}} = -0.4\,\mathrm{V}$.

Fig. 5(a) shows the channel length (l_{ch}) dependence of the STHS for various gate oxide thicknesses t_{ox}. For very short tubes below 7 nm direct tunneling between source and drain significantly contributes to the current leading to a very high STHS. Between 7 nm and 15 nm the STHS depends on the thickness of the barrier which changes with the tube length and above 15 nm the shape of the barrier is bias independent for the relevant gate voltages and the STHS is determined by the amount of current flowing above the barrier under the gate. Since this barrier is fixed by the electrostatics of the device, the STHS approaches the thermionic limit for devices with a very good channel control albeit the magnitude of the current is low since it must tunnel through the bias-independent near-contact barrier.

Fig. 5(b) confirms the impact of the device electrostatics on the device behavior. The thinner the gate oxide, the lower is the STHS of the device. The theoretical predictions of the STHS suggest that the negative impact of near-contact barriers may be partially suppressed by excellent gate control paving the way to very short channel devices.

Interestingly, the nominal value of the Schottky barrier height (as defined in Fig. 1(b)) does not influence the scaling behavior significantly. Fig. 5(c) shows the related simulation results for various nominal barrier heights and two different oxide thicknesses. This observation emphasizes the importance of the barriers formed by the injected charges. Thus, a balance between the amount of carriers which leak into the channel band gap and which are responsible for the near-contact barriers and the total amount of current flowing through the device must be found. This balance depends considerably on the details of the fabrication process and the materials employed for the contact formation.

In addition, the simulation study also confirms that the neglect of the tube charge for the calculation of the STHS as proposed in [18] does not correctly capture scaling behavior since near-contact barriers cannot be formed without charges.

Further simulations for various drain-voltages not shown here reveal two additional interesting observations. The logarithmically scaled transfer characteristic as shown in Fig. 2 is shifted along the gate voltage axis if the drain voltage is changed. The observation is also verified by the experimental results in [5]. The amount of the shift crucially depends on the overall electrostatics (i. e. on the source-drain separation and the gate oxide). For short channels and a relatively thick oxide, the impact of the drain potential on the potential barrier nearby the source contact region is high leading to a significant shift of the logarithmic scaled transfer characteristic towards higher gate voltages. The impact of the drain voltage on the source-sided potential barrier (i.e. on the current flow dominating barrier) is also known as drain-induced barrier lowering. However, the here observed DIBL does not imply a lack of current saturation (a claim referenced in the introduction which we could not confirm) since the STHS is evaluated for positive and small negative voltages whereas the output characteristic is evaluated for high negative voltages which fix the shape of the source-sided potential barrier in the energy interval relevant for charge injection.

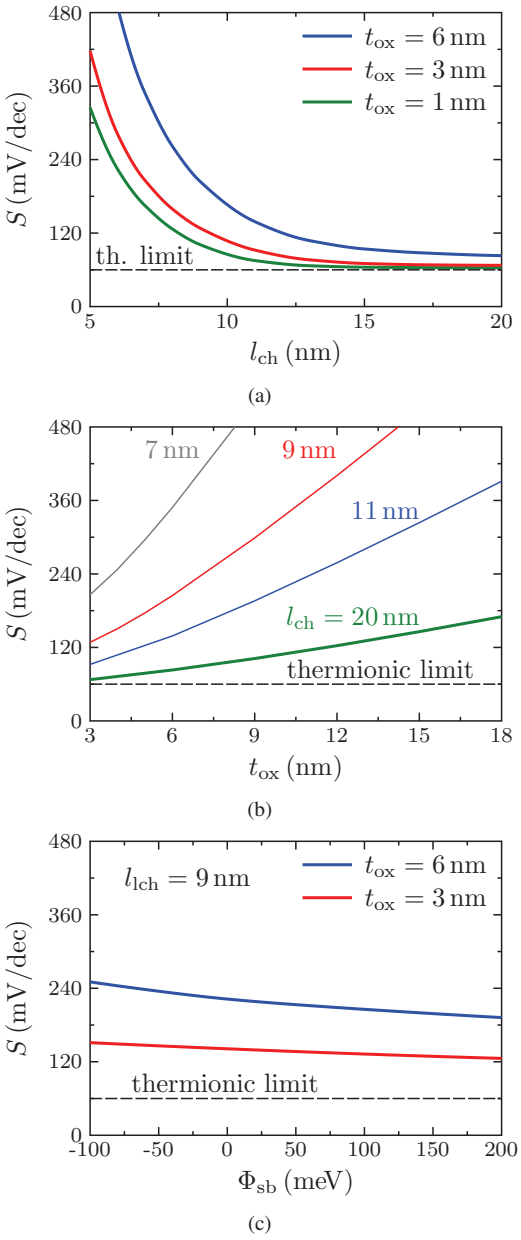

Fig. 5: Subthreshold slope S for **(a)** various channel lengths, **(b)** several oxide thicknesses and **(c)** different Schottky barrier heights. The STHS in these figures was extracted for $V_{gs} = 0\,V$ and $V_{ds} = -0.4\,V$.

IV. Conclusion

The STHS in short channel CNTFETs is found to be determined by tunneling phenomena through near-contact barriers instead of the thermionic current above the barriers. Since these barriers depend on the charge injection, i. e. the coupling strengths and the Schottky barrier height, the STHS is sensitive to changes of these parameters which must be modeled with care. For predictive modeling, however, a direct link between the parameters of the heterojunction contact model and more rigor atomistic simulations needs to be established.

In addition to an optimized contact, a well-balanced electrostatics is needed to get reasonable values for the STHS for very short CNTFET channels.

Acknowledgment

The authors acknowledge the Cfaed, the DFG project CL384/2-1 and the NAMITEC. The authors are also indebted to Prof. J. Knoch for valuable discussions.

References

[1] S. Hasan, S. Salahuddin, M. Vaidyanathan, and M. A. Alam, "High-frequency performance projections for ballistic carbon-nanotube transistors," *IEEE Trans. on Nanotechnology*, vol. 5, no. 1, pp. 14–22, 2006.

[2] M. Claus, S. Blawid, P. Sakalas, and M. Schröter, "Analysis of the frequency dependent gate capacitance in cntfets," in *Proc. SISPAD*, 2012, pp. 336–339.

[3] M. Claus, S. Blawid, S. Mothes, and M. Schröter, "High-frequency ballistic transport phenomena in schottky-barrier cntfets," *IEEE Trans. on Electron Devices*, vol. 59, no. 10, pp. 2610–2618, 2012.

[4] M. Schroter, M. Claus, P. Sakalas, M. Haferlach, and D. Wang, "Carbon Nanotube FET Technology for Radio-Frequency Electronics: State-of-the-Art Overview," *IEEE Journal of the Electron Devices Society*, vol. 1, no. 1, pp. 9–20, 2013.

[5] A. D. Franklin, M. Luisier, S.-J. Han, G. Tulevski, C. M. Breslin, L. Gignac, M. S. Lundstrom, and W. Haensch, "Sub-10 nm carbon nanotube transistor," *Nano Letters*, vol. 12, no. 2, pp. 758–762, 2012.

[6] F. Léonard and D. A. Stewart, "Properties of short channel ballistic carbon nanotube transistors with ohmic contacts," *Nanotechnology*, vol. 17, no. 18, p. 4699, 2006.

[7] J. Guo, S. Datta, and M. Lundstrom, "A numerical study of scaling issues for schottky-barrier carbon nanotube transistors," *IEEE Trans. on Electron Devices*, vol. 51, no. 2, pp. 172–177, 2004.

[8] A. W. Cummings and F. Leonard, "Enhanced performance of short-channel carbon nanotube field-effect transistors due to gate-modulated electrical contacts," *ACS Nano*, vol. 6, no. 5, pp. 4494–4499, 2012.

[9] N. Nemec, D. Tomcanek, and G. Cuniberti, "Modeling extended contacts for nanotube and graphene devices," *Physical Review B*, vol. 77, pp. 125 420 – 125 432, 2008.

[10] H.-N. Nguyen, D. Querlioz, A. Bournel, S. Retailleau, and P. Dollfus, "Ohmic and schottky contact cntfet: Transport properties and device performance using semi-classical and quantum particle simulation," in *Semiconductor-On-Insulator Materials for Nanoelectronics Applications*, ser. Engineering Materials, A. Nazarov, J.-P. Colinge, F. Balestra, J.-P. Raskin, F. Gamiz, and V. Lysenko, Eds. Springer Berlin Heidelberg, 2011, pp. 215–235.

[11] M. Claus, S. Mothes, and M. Schröter, "About the charge injection limitation in Schottky barrier CNTFETs (accepted for publication)," in *International Semiconductor Conference Dresden - Grenoble (ISCDG)*, 2013.

[12] M. Claus, D. Gross, M. Haferlach, and M. Schröter, "Critical review of cntfet compact models," in *NSTI-Nanotech (Workshop on Compact modeling)*, vol. 2, 2012, pp. 770–775.

[13] J. Svensson and E. E. B. Campbell, "Schottky barriers in carbon nanotube-metal contacts," *Journal of Applied Physics*, vol. 110, no. 11, p. 111101, 2011.

[14] J. Knoch and J. Appenzeller, "Tunneling phenomena in carbon nanotube field-effect transistors," *physica status solidi (a)*, vol. 205, no. 4, pp. 679–694, 2008.

[15] N. Paydavosi, K. D. Holland, M. M. Zargham, and M. Vaidyanathan, "Understanding the frequency- and time-dependent behavior of ballistic carbon-nanotube transistors," *IEEE Trans. on Nanotechnology*, vol. 8, no. 2, pp. 234–244, 2009.

[16] S. Blawid, M. Claus, and M. Schröter, "Phenomenological modeling of charge injection - beyond the schottky barrier paradigm," in *27th Symposium on Microlelectronics Technology and Devices (SBMicro), ECS Transactions*, vol. 49, Brasília, 2012, pp. 85–92.

[17] S. Selberherr, *Analysis and simulation of semiconductor devices*. Springer-Verlag, 1984.

[18] S. Heinze, M. Radosavljević, J. Tersoff, and P. Avouris, "Unexpected scaling of the performance of carbon nanotube schottky-barrier transistors," *Physical Review B*, vol. 68, p. 235418, 2003.